FM

NATIONAL AERONAUTICS AND SPACE ADMINISTRATION

MSC INTERNAL NOTE NO. 69-FM-227

September 23, 1969

Technical Library, Bellcomm, Inc.

FEB 9 1970

GUIDANCE ANALYSIS OF ENTRY CORRIDORS FOR AERODYNAMIC BRAKING INTO ORBIT AROUND MARS OR VENUS

Internal Note No. 69-FM-227

(NASA-TM-X-69727) GUIDANCE ANALYSIS OF ENTRY CORRIDORS FOR AERODYNAMIC BRAKING INTO ORBIT AROUND MARS OR VENUS (NASA) 36 p

N74-70883

Unclas
00/99 16314

Advanced Mission Design Branch

MISSION PLANNING AND ANALYSIS DIVISION

MANNED SPACECRAFT CENTER
HOUSTON, TEXAS

MSC INTERNAL NOTE NO. 69-FM-227

PROJECT APOLLO

GUIDANCE ANALYSIS OF ENTRY CORRIDORS FOR AERODYNAMIC BRAKING INTO ORBIT AROUND MARS OR VENUS

By Benjamine J. Garland
Advanced Mission Design Branch

September 23, 1969

MISSION PLANNING AND ANALYSIS DIVISION
NATIONAL AERONAUTICS AND SPACE ADMINISTRATION
MANNED SPACECRAFT CENTER
HOUSTON, TEXAS

Approved: Jack Funk
Jack Funk, Chief
Advanced Mission Design Branch

Approved:
John P. Mayer, Chief
Mission Planning and Analysis Division

CONTENTS

GUIDANCE ANALYSIS OF ENTRY CORRIDORS FOR AERODYNAMIC BRAKING INTO ORBIT AROUND MARS OR VENUS

By Benjamine J. Garland

1.0 SUMMARY

A guidance system for use of aerodynamic braking of a spacecraft is described. The guidance equations attempt to control the apoapsis altitude and inclination of the trajectory after the spacecraft skips from the atmosphere by a roll of the spacecraft. A propulsion system is required to change the skip trajectory to the target orbit.

This guidance system was used to evaluate the feasibility of aerodynamic braking being used for entry speeds of between 18 000 fps and 26 000 fps at Mars and between 36 000 fps and 46 000 fps at Venus. The assumed spacecrafts had lift-to-drag (L/D) ratios of 0.5 and 1.0 at Mars. The spacecraft for Venus had an L/D of 1.0. The ballistic coefficient (W/C_DS) was 100 psf for the 0.5-L/D spacecraft. The 1.0-L/D spacecraft had a ballistic coeffieient of between 100 psf and 1000 psf. The feasibility of aerodynamic braking being used for the higher velocities at Venus is questionable. The use of the aerodynamic braking maneuver does appear to be feasible at Mars.

2.0 INTRODUCTION

Previous studies (ref. 1) have shown that the initial size of an interplanetary spacecraft can be reduced significantly if the atmosphere of the target planet is used to decrease the velocity of the spacecraft. The aerodynamic forces developed by the spacecraft are used to change the trajectory from the hyperbolic approach path to an elliptic path that has a specified apoapsis altitude. The most efficient place to use the propulsion system is near the apoapsis to raise the periapsis above the sensible atmosphere. If for some reason the desired apoapsis is not obtained, it will be corrected by a change in the periapsis velocity.

A guidance system described in reference 2 was used to study the feasibility of aerodynamic braking being used to establish an orbit at

Mars. The assumed spacecraft had an L/D of 0.5 and a W/C_DS of 120 psf. The entry speed was varied between 17 000 fps and 20 000 fps.

The study has been extended to include aerodynamic braking at Venus and higher entry speeds at Mars. The entry speeds at Venus are between 36 000 fps and 46 000 fps. The entry speeds at Mars are between 18 000 fps and 26 000 fps. Another class of spacecraft was also considered. This spacecraft has an L/D of 1.0 and a W/C_DS of 100 psf to 1000 psf. It was necessary to modify the guidance logic used in reference 2 because of the wider range of operating conditions.

The results of the study of the entry corridors at Mars and Venus are included in this report. The flow diagrams of the guidance system and the values of the guidance constants are presented in the appendix.

3.0 SYMBOLS

C_D	drag coefficient, n.d.
D	drag, lb
g_E	acceleration of gravity at surface of Earth, 32.2 fps
h	altitude, ft or n. mi.
L	lift, lb
S	reference area, ft^2
V	velocity, fps
W	weight, lb
γ	flight-path angle, deg or rad
ΔV_T	total velocity required to establish the target orbit, fps
ρ	density, $lb\text{-}sec^2/ft^4$

Subscripts

en entry

p periapsis

4.0 METHOD

4.1 Description of Maneuver to Establish Orbits

The sequence of maneuvers used to establish the orbit is shown in figure 1. The spacecraft approaches the planet along a hyperbolic path which must intersect the atmosphere within certain limits known as the entry corridor. The purpose of the atmospheric phase is to decrease the speed of the spacecraft and to deflect its path so that it leaves the atmosphere along a trajectory with the desired apoapsis altitude. The periapsis of the spacecraft's orbit is raised above the atmosphere by an increase in the spacecraft's apoapsis velocity. In actual practice, the apoapsis altitude of the exit trajectory will not equal the apoapsis altitude of the target orbit. Therefore, the apoapsis altitude will be adjusted by a change in the velocity at the periapsis of the intermediate orbit. The depth of the entry corridor and the total velocity change required to establish the target orbit (ΔV_T) are two convenient measures of the performance of the combined spacecraft and guidance system.

A more detailed description of the atmospheric phase is shown in figure 2. The beginning and end of this phase are defined by arbitrary values of the acceleration of the spacecraft caused by aerodynamic forces. The atmospheric phase is divided into three phases by the guidance system. These subdivisions are the transition to a constant altitude, the constant altitude phase, and the exit phase.

4.2 Description of Guidance System

The guidance equations were developed in reference 2 and the flow diagrams of the guidance logic are presented in the appendix. This section is limited to a brief description of the guidance system.

The guidance system assumes that the spacecraft produces a constant value of L/D and that the only method used to control the spacecraft is to roll the vehicle. The guidance uses approximate analytic solutions to the equations of motion to determine the required roll angle. This technique is typical of closed-form prediction guidance schemes.

The basic arrangement of the guidance logic is shown in figure 3. The guidance commands are based on the changes in the velocity measured by the inertial measurment unit (IMU). In the navigation section, the

output of the IMU is used to calculate the position and velocity of the spacecraft. Basically, the navigation equations are the same as those used for the Apollo guidance (ref. 3) and are used once during each cycle through the computer.

The mode selector's only purpose is to direct the computations to the correct section of the guidance logic. The lift vector of the spacecraft is pointed downward during the approach phase which ends whenever the measured acceleration along the velocity vector exceeds 1.6 ft/sec^2 ($0.05g_E$, where g_E is the gravitational acceleration at the surface of the Earth).

The transition phase attempts to guide the spacecraft to a constant altitude path. The guidance equations for this phase are based on the results of reference 4, although the derived equations are different. The L/D given by the guidance equation is used except for three cases. The first exception, a result of numerical inaccuracy, is when the estimated density at the beginning of the constant altitude phase is less then the current calculated density. The remaining two conditions are that the estimated acceleration at the beginning of the constant altitude phase is greater than the maximum allowable acceleration and that the constant altitude path lies below the minimum permissible altitude. The guidance will call for full positive lift if any of these three situations exist. The transition phase continues until the estimated time remaining before the path is horizontal is less than the time required to roll the space-through 180°.

The purpose of the constant altitude phase is to allow the spacecraft to decelerate until the exit phase can be flown successfully. Therefore, a portion of the computations for the exit phase must be performed each cycle although the spacecraft is being guided along a constant altitude path. The constant altitude phase continues until the target apoapsis altitude can be reached by use of a constant value of L/D which is less than some arbitrary value.

The exit phase guidance equations are based on the second-order solution to the equations of motion presented in reference 5. The second-order solution is used to calculate the apoapsis altitude achieved by use of a constant value of L/D, and the correct value of L/D is found by use of a Newton-Raphson iteration scheme. A combination of the previous computed value of L/D and the current value is used to steer the spacecraft. The exit phase ends whenever the measured acceleration along the velocity vector becomes less than $0.05g_E$. The aerodynamic braking maneuver is completed at this point.

The inclination of the orbit is controlled by the direction of the roll angle. It is assumed that the change in the inclination of the orbit is approximated by the change in the spacecraft's heading. The approximate change in heading is given in reference 7. The estimate of the change in inclination during the atmospheric phase is compared to the desired inclination to determine the direction of roll.

5.0 NUMERICAL APPLICATION AND RESULTS

A four-degree-of-freedom digital trajectory program was used to evaluate the performance of the combined guidance and spacecraft system. A spherical rotating planet is assumed for the trajectory program. The physical properties of Mars and Venus are given in references 7 and 8, respectively. The models of the atmosphere of Mars presented in reference 9 and the models presented in reference 10 for Venus were used in the study. The variation of the atmospheric density with altitude of the three atmospheric models for Mars and the two models for Venus are presented in figure 4.

The nominal characteristics of the control system are as follows.

Maximum roll rate, deg/sec	±20
Roll acceleration, deg/sec^2	±10
Roll deadband, deg	±4

The control system characteristics are those of the Apollo command module.

Two basic spacecraft were considered in this study. The L/D and W/C_DS of these spacecraft and the range of entry velocities are listed in the following table. The initial altitudes were 300 000 feet at Mars and 600 000 feet at Venus.

Planet	L/D	W/C_DS, psf	V_{en}, fps
Mars	0.5	100	18 000 to 26 000
Mars	1.0	100 to 1000	18 000 to 26 000
Venus	1.0	100 to 1000	36 000 to 46 000

The 0.5-L/D spacecraft is typical of the type that could be used to land on the surface of the planet. Because manned landings on the surface of Venus are extremely unlikely, the performance of this spacecraft

was considered only at Mars. The velocities include a realistic range of entry velocities at each planet.

The top and bottom of the entry corridor can be designated by either the altitude of the periapsis of the approach trajectory or by the flight-path angle at some arbitrary altitude. The top of the entry corridor is defined as the maximum periapsis altitude or shallowest entry angle at which the guidance has the capability to steer the spacecraft to the target apoapsis altitude. The bottom of the entry corridor is defined by three different criteria. The first definition of the bottom of the entry corridor is the point at which the spacecraft is subjected to an acceleration of $10g_E$. The bottom of the entry corridor can also be defined as the periapsis altitude of entry angle when the minimum allowable altitude of 50 000 feet. The last definition is based on the ΔV_T. A typical variation of ΔV_T with respect to γ_{en} is shown in figure 5. The ΔV_T decreases rapidly as γ_{en} is increased from -13° to -12°. The ΔV_T remains between 120 fps and 200 fps until γ_{en} is increased to -7°. The ΔV_T at -6.8° is 1400 fps and falls outside the figure. The bottom of the entry corridor is defined as the point at which ΔV_T begins to increase rapidly as the periapsis altitude is lowered. This definition is more nebulous than the first two definitions.

The entry corridor at Venus is presented in figure 6 for the high density atmosphere model. The depth of the entry corridor is 22.0 n. mi. if the W/C_DS is 1000 psf and if V_{en} is 36 000 fps. The top of the entry corridor is practically independent of the entry velocity.

The effect of the low density atmosphere on the entry corridor at Venus is shown in figure 7. The change in the atmospheric models will lower the top of the entry corridor to 42.4 n. mi. for a W/C_DS is 1000 psf. The corridor depth is changed less than 2.0 n. mi. The top of the entry corridor is almost independent of V_{en}. The bottoms of the entry corridors were determined by the $10g_E$ acceleration limit. The maximum dynamic pressure was 7300 psf for a W/C_DS of 1000 psf and the high density atmosphere. The minimum altitude was 188 000 feet for a W/C_DS of 1000 psf and the low density atmosphere. The ΔV_T for a target orbit with a periapsis altitude of 200 n. mi. and an apoapsis altitude of 10 000 n. mi. was between 100 fps and 200 fps. More than half of the ΔV_T was applied at the apoapsis of the exit trajectory.

The entry corridor into the mean density atmosphere at Mars is shown in figure 8 for V_{en} from 18 000 fps to 26 000 fps. The L/D is 1.0, and W/C_DS is 100 psf, 500 psf, and 1000 psf. The maximum variation of the top of the entry corridor is 2.0 n. mi. over the range of V_{en}. The top of the corridor is the lowest at the highest V_{en} and is 29.4 n. mi., 21.7 n. mi., and 18.3 n. mi. for W/C_DS of 100 psf, 500 psf, and 1000 psf, respectively. All three definitions of the bottom of the corridor are represented in this figure. The bottom of the entry corridor is defined by the minimum altitude of 50 000 feet if W/C_DS equals 500 psf or 1000 psf. The minimum corridor depth is 21.5 n. mi. if W/C_DS is 1000 psf and increases to 32.5 n. mi. when W/C_DS is decreased to 500 psf. If W/C_DS is 100 psf, the bottom of the entry corridor is defined by the maximum acceleration of $10g_E$ if V_{en} is greater than 22 300 fps. If V_{en} is less than 22 300 fps, the bottom of the entry corridor is defined by the increase in ΔV_T. The maximum entry corridor depth is 65.0 when V_{en} is equal to 22 300 fps. The minimum corridor depth is 24.6 n. mi. at the slowest V_{en}.

The entry corridor at Mars for the three atmospheric models is presented in figure 9. The L/D is 1.0, and W/C_DS is 1000 psf. The entry corridor at Venus was raised or lowered by changes in the atmospheric model, but the corridor depth was essentially unaffected. The top of the entry corridor at Mars is lowered, and the bottom of the entry corridor is raised if the density is decreased. The minimum corridor depth in the low density atmosphere is 9.2 n. mi. for a V_{en} of 26 000 fps. The corridor depth at this velocity is 56.0 n. mi. for the high density atmosphere.

A decrease in L/D to 0.5 will cause the top of the entry corridor at Mars to be decreased between 0.6 and 2.8 n. mi. as shown in figure 10. At the same time, the bottom of the entry corridor will be increased between 5.4 and 36.5 n. mi. These results occur for the mean density atmosphere and for a W/C_DS of 100 psf. The bottom of the entry is determined by the increase in V_T over the entire velocity range. The minimum entry corridor depth is 11.0 when V_{en} is 18 000 fps. The corridor depth increases to a maximum of 36 n. mi. as V_{en} is increased to 26 000 fps.

The depth and location of the entry corridor at Mars change as the atmosphere is changed. The entry corridors for the three atmospheric models are shown in figure 11 for a L/D of 0.5 and a W/C_DS of 100 psf.

The entry corridor for the mean density atmosphere is the same as was shown in figure 10 and is used for comparison. If V_{en} is 26 000 fps, the depth of the entry corridor for the high density atmosphere is increased by 4.5 n. mi., and the top of the entry corridor is raised by 12.0 mi. The corridor depth is decreased by 3.0 n. mi., and the top of the entry corridor is lowered by 7.0 n. mi. when the low density atmosphere is assumed. Changes in the atmosphere have less effect as the V_{en} is decreased.

The maximum dynamic pressure during any entry within the corridor at Mars was 12 000 psf, and the maximum acceleration was $10g_E$. The ΔV_T for a target apoapsis altitude of 10 000 n. mi. and a target periapsis altitude of 200 n. mi. was between 100 and 200 fps except for the low L/D spacecraft in the dense atmosphere. In this case, the ΔV_T increased rapidly at the lower V_{en} and was between 400 fps and 500 fps at the lowest value considered.

A study of the approach navigation and guidance corridor at Mars and Venus was reported in reference 11. The depth of the approach guidance corridor at Venus is approximately equal to the depth of the entry corridor when V_{en} is 46 000 fps. The depth of the entry corridor increases as V_{en} is decreased, while the depth of the guidance corridor decreases. Except for the entry of a 1.0 L/D with a W/C_DS of 1000 psf into the low density atmosphere, the entry corridors at Mars are several times as large as the approach guidance corridors. It should be mentioned that the entry corridor depths are optimistic because the study does not consider errors such as those which occur in the initial position and velocity, in the IMU, or in the vehicle characteristics. The depth of the entry corridor will be decreased by any errors which may occur.

The flexibility of the guidance was demonstrated by the variety of cases considered. The only parameters that were changed in the guidance were the following: (1) the planet's radius, spin rate, and gravitational constant; (2) the L/D and W/C_DS of the spacecraft; and (3) the exponential decay rate of the atmosphere. The guidance equations were used satisfactorily for the cases considered.

6.0 CONCLUDING REMARKS

The proposed guidance system for aerodynamic braking into a planetary orbit has the capability to perform satisfactorily over a wide range of conditions at both Mars and Venus with no changes except those that describe the physical properties of the planet or the spacecraft.

The guidance was used to evaluate the entry corridors at Mars and Venus for spacecraft with an L/D of 0.5 or 1.0. The W/C_DS of the 0.5-L/D spacecraft was 100 psf, and the W/C_DS of the 1.0-L/D spacecraft was between 100 psf and 1000 psf. The entry velocity at Mars was from 18 000 fps to 26 000 fps. The entry velocity at Venus was between 36 000 fps and 46 000 fps. The use of aerodynamic braking at Mars appears to be possible, but its use at Venus is doubtful at the higher values of entry velocity.

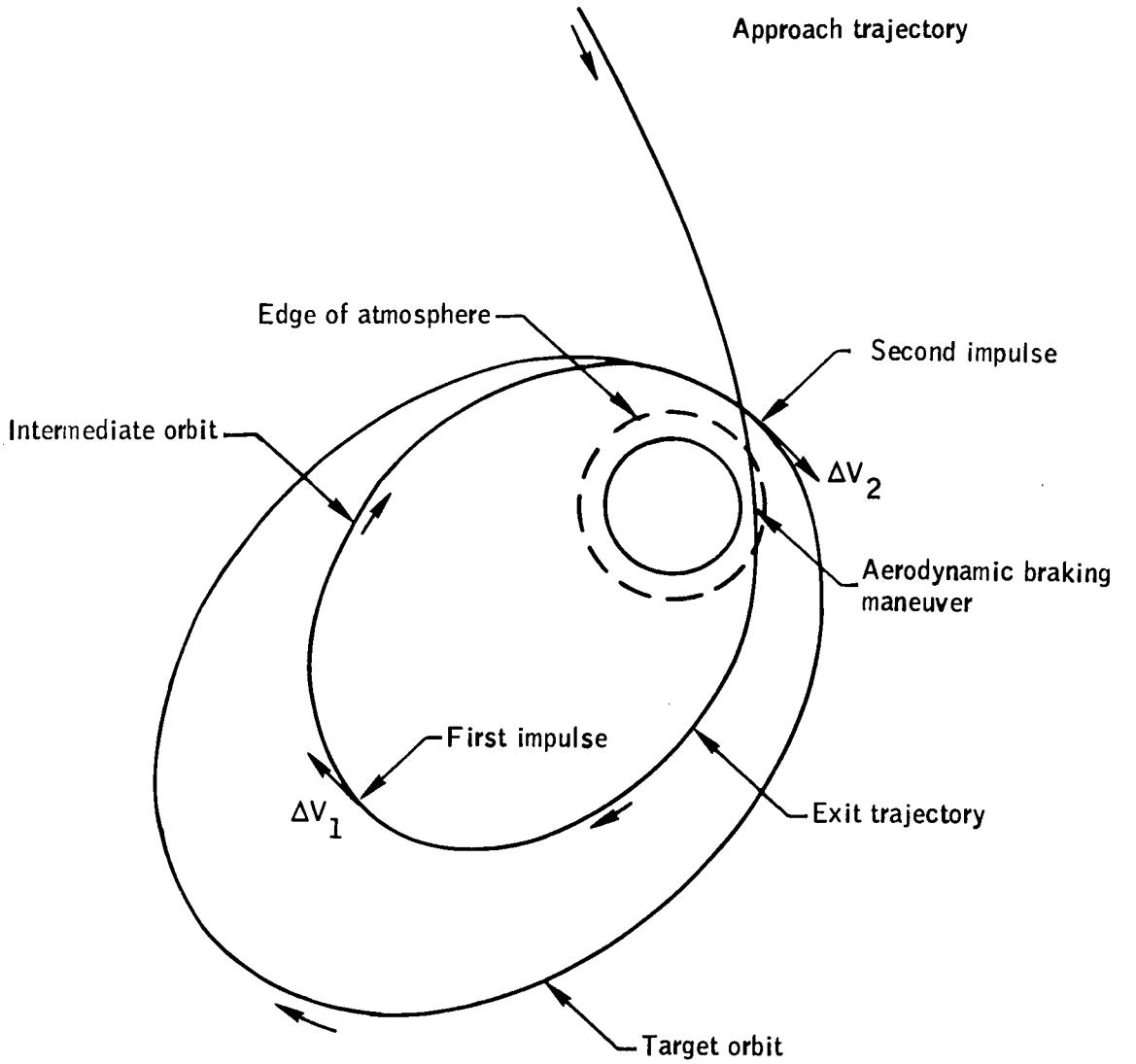

Figure 1.- Sequence of maneuvers necessary to establish target orbit.

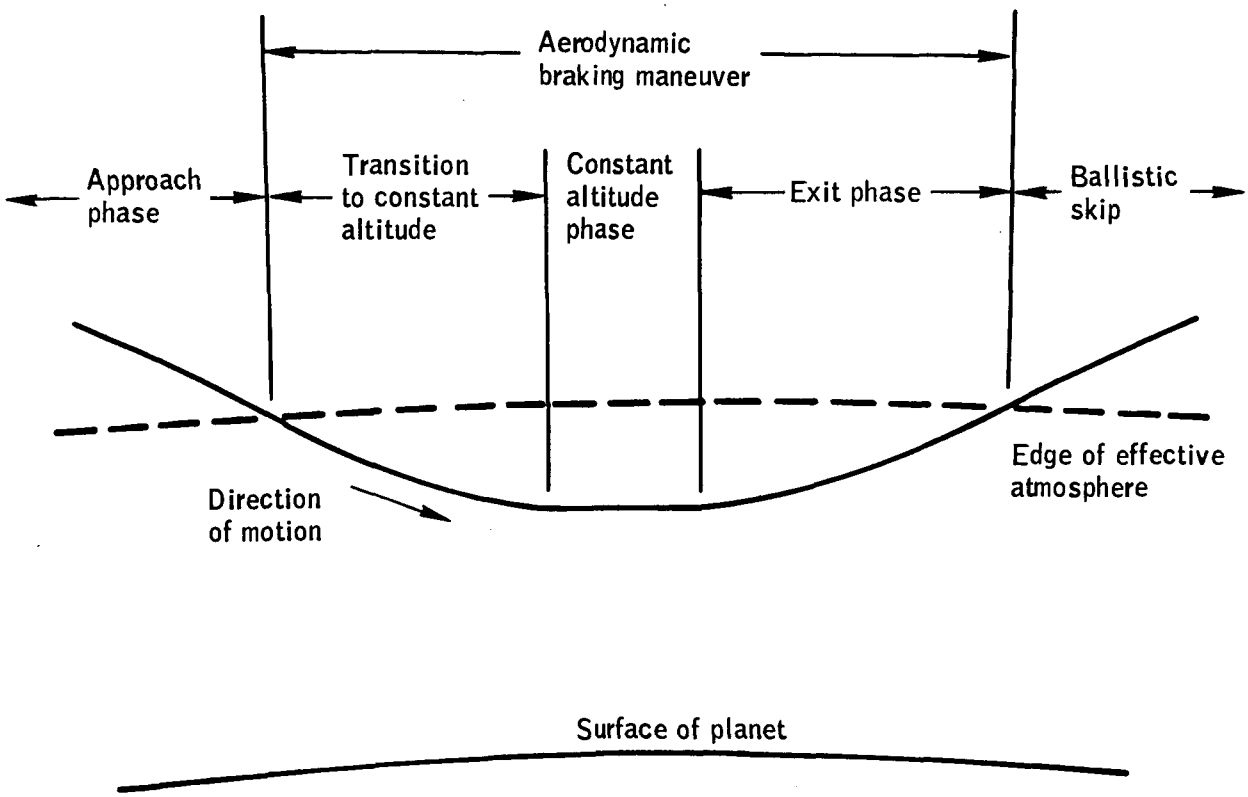

Figure 2.- Phases of aerodynamic braking maneuver.

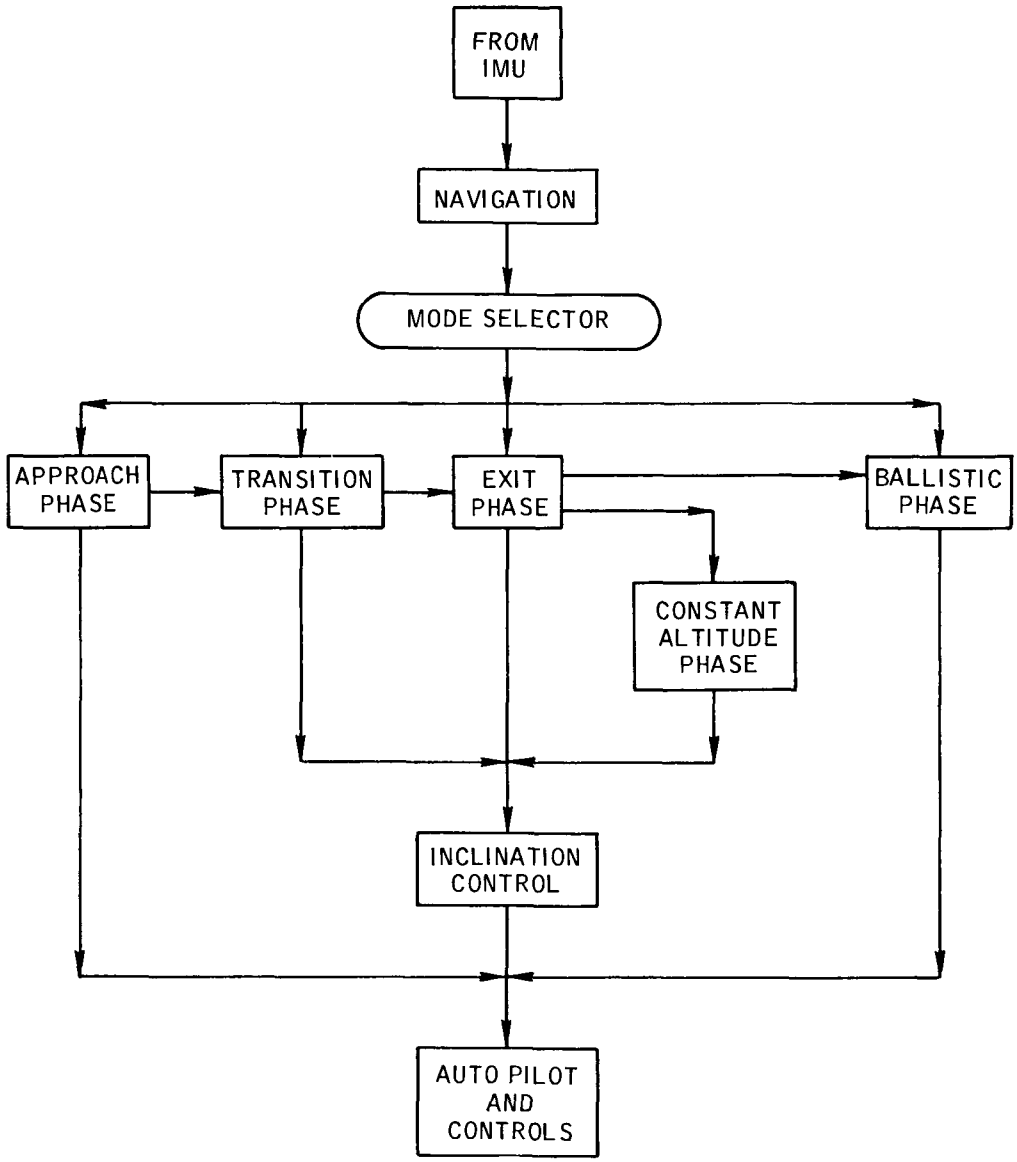

Figure 3.- Basic logic of guidance.

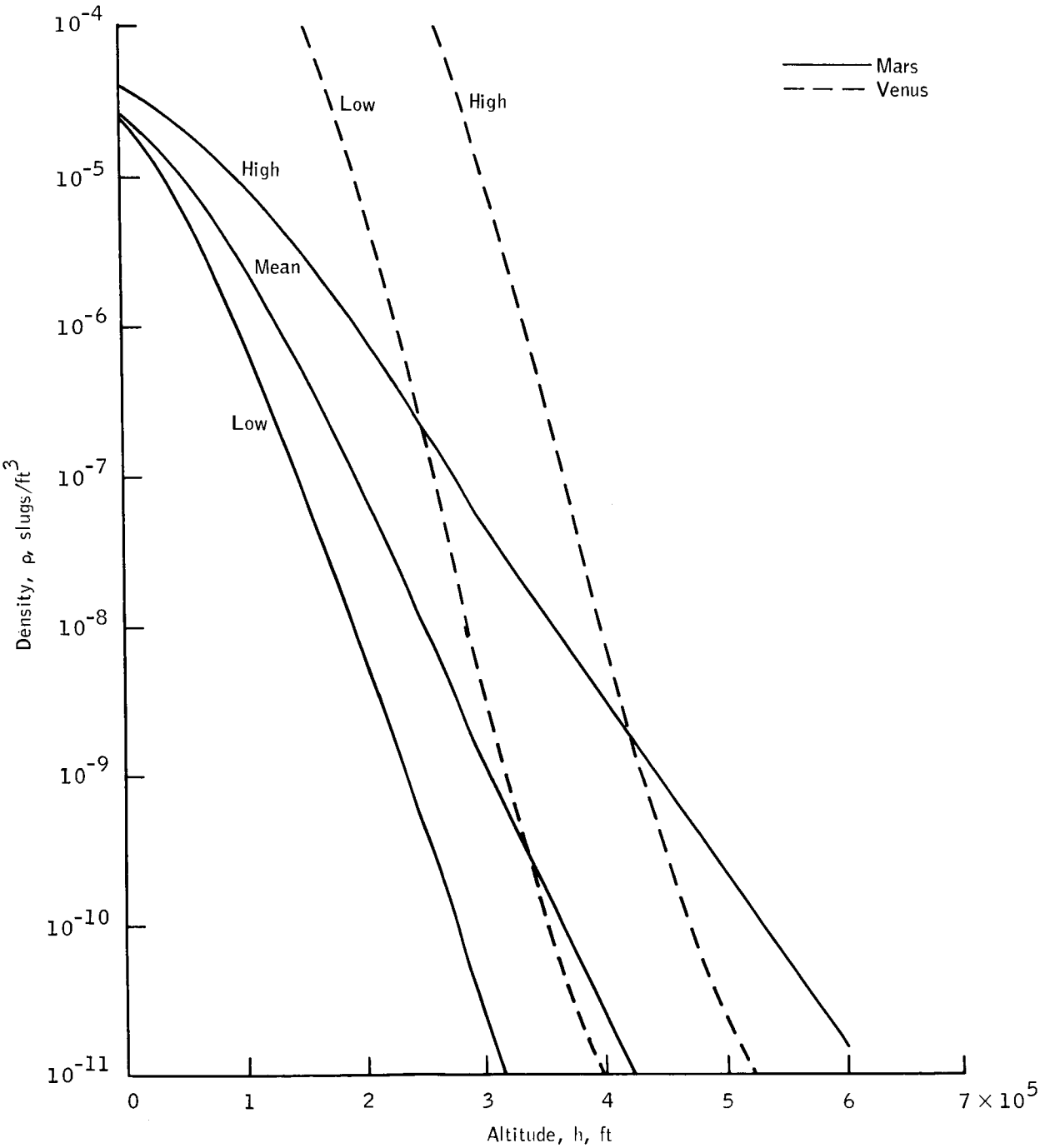

Figure 4.- Atmospheric models used in study.

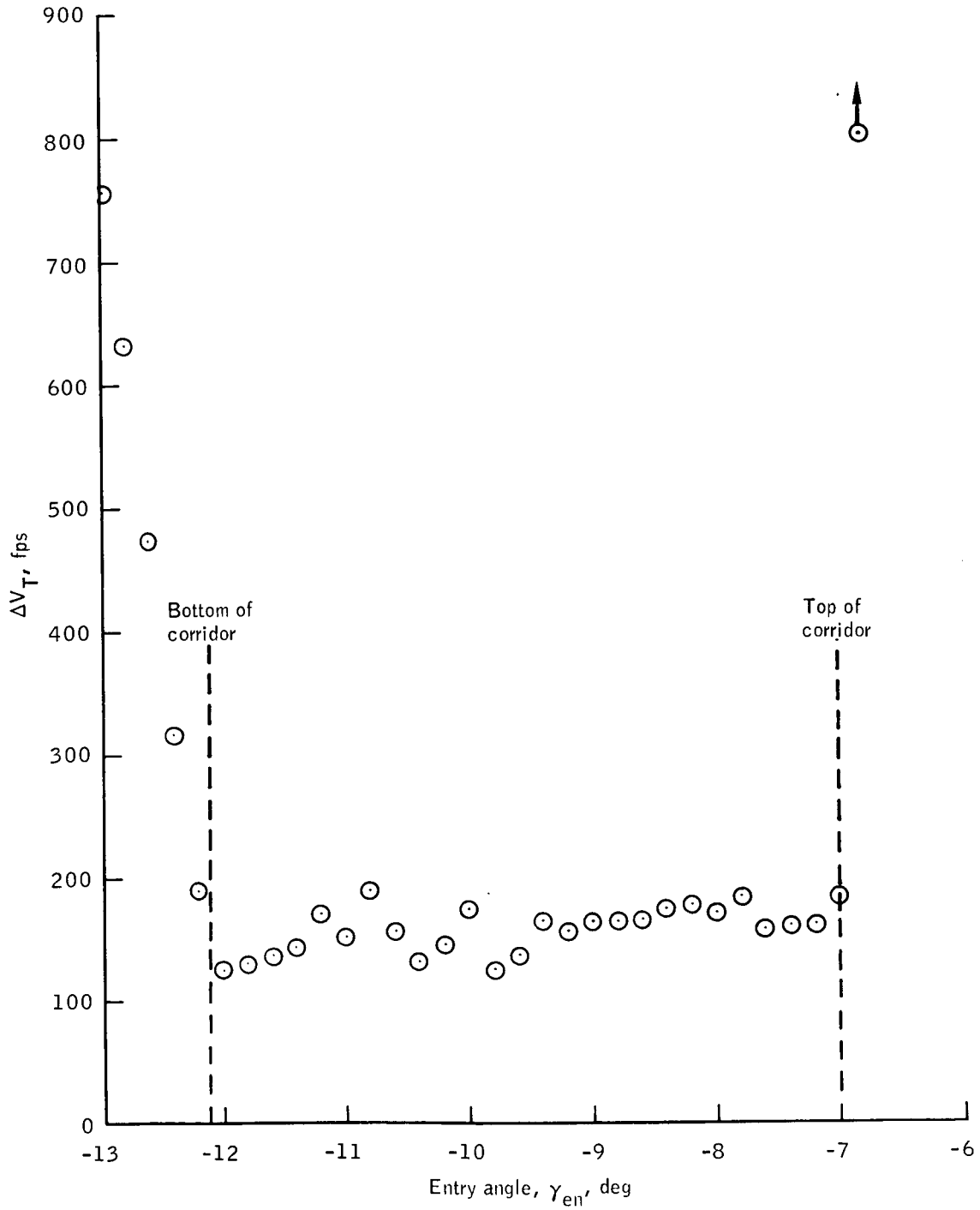

Figure 5.- Definition of corridor limits by use of ΔV_T.

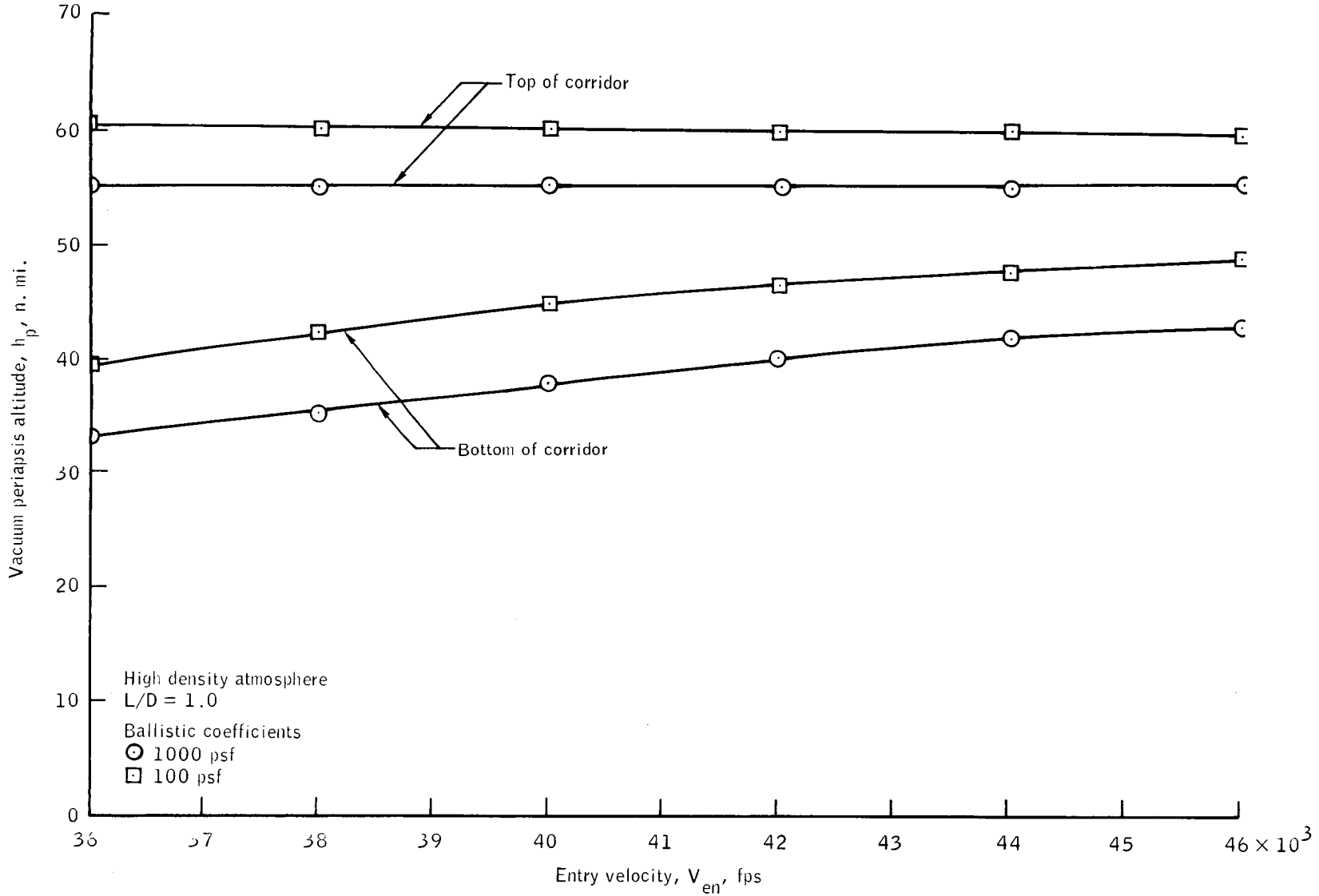

Figure 6.- Entry corridor for high density atmosphere at Venus (L/D = 1.0, W/C_DS = 100, 1000 psf).

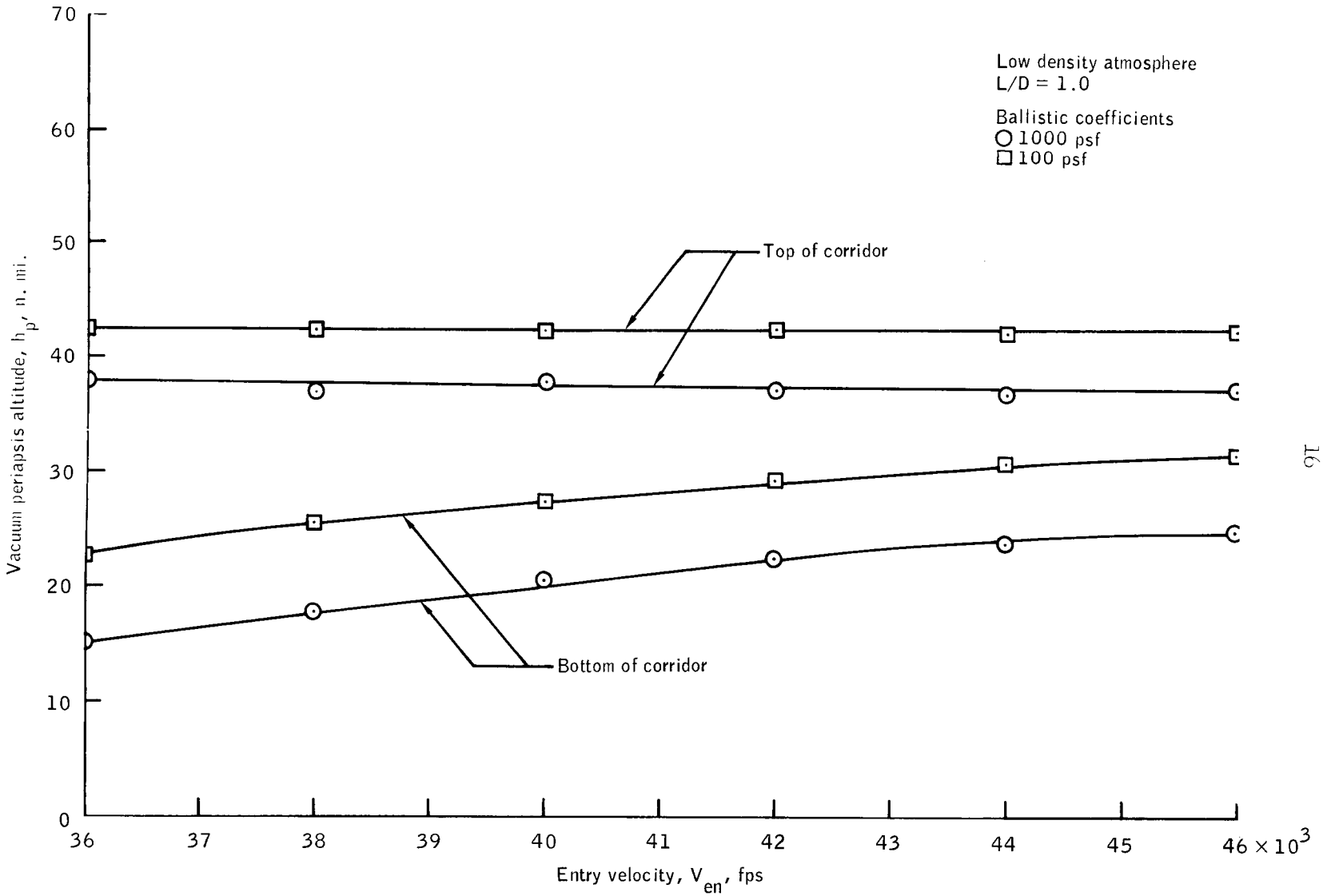

Figure 7.- Entry corridor for low density atmosphere at Venus (L/D = 1.0, $W/C_D S$ = 100 1000 psf).

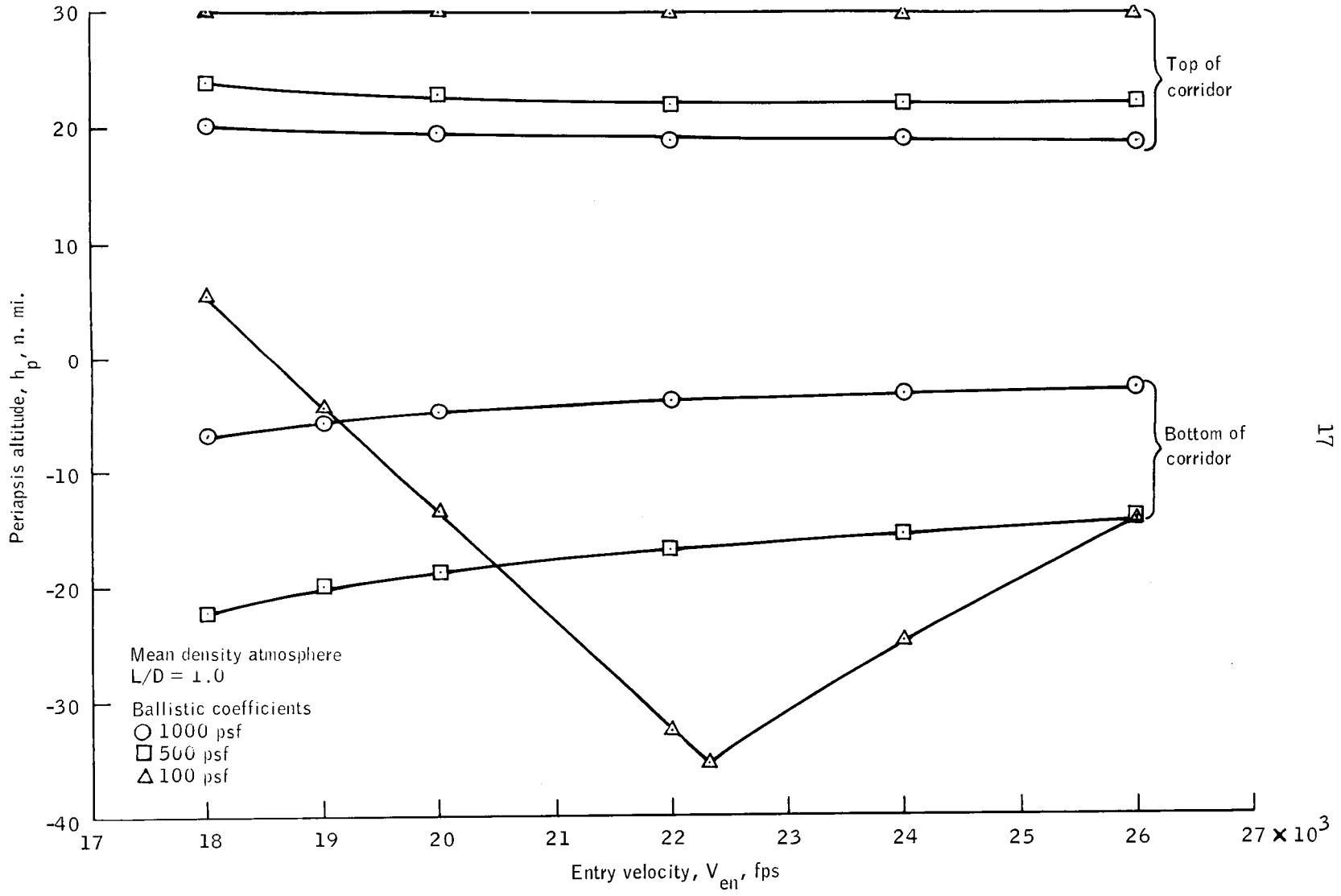

Figure 8.- Entry corridor into mean density atmosphere at Mars (L/D = 1.0, W/C_DS = 100, 500, 1000 psf).

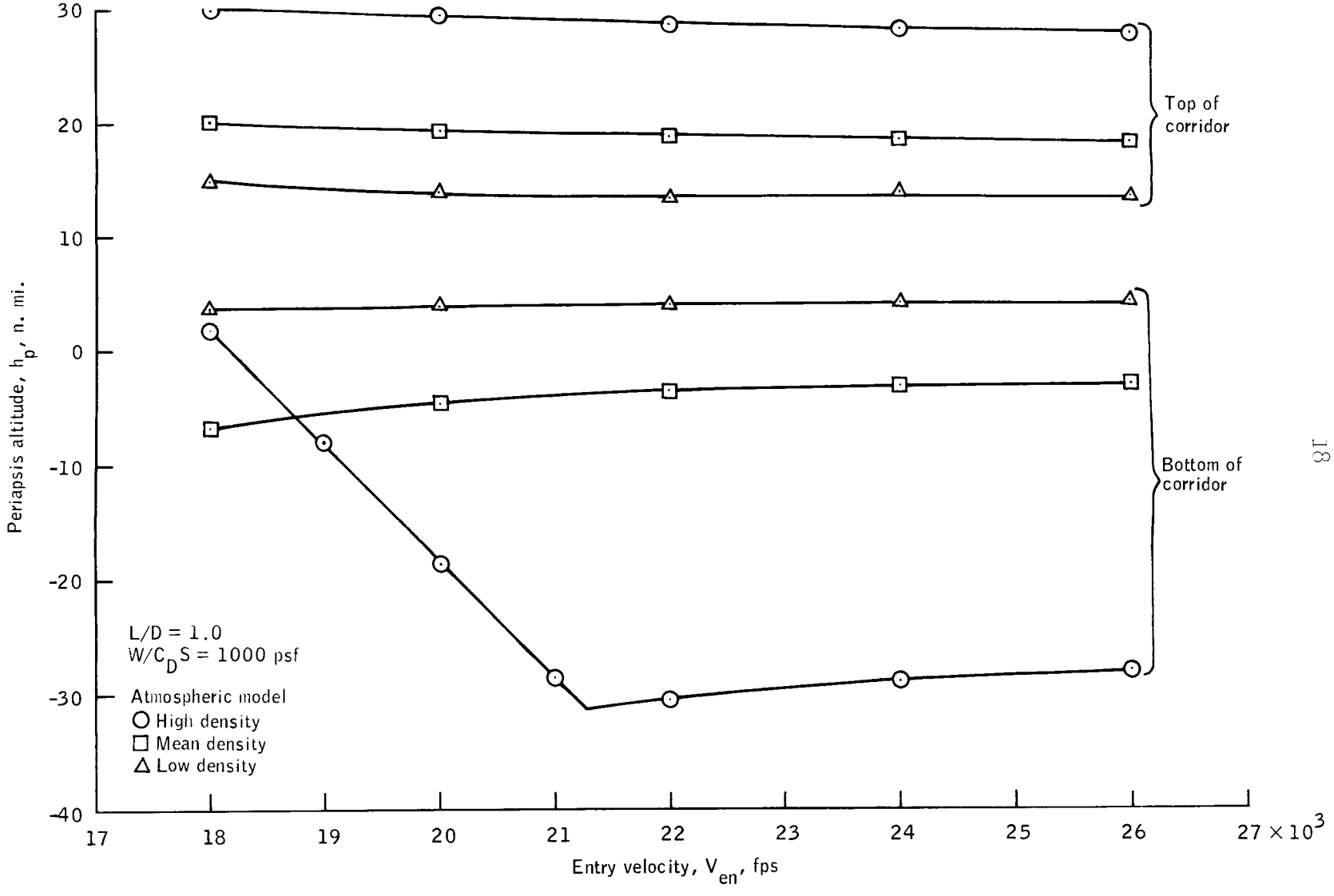

Figure 9.- Effect of atmospheric models on entry corridor at Mars (L/D = 1.0, W/C_DS = 100 psf).

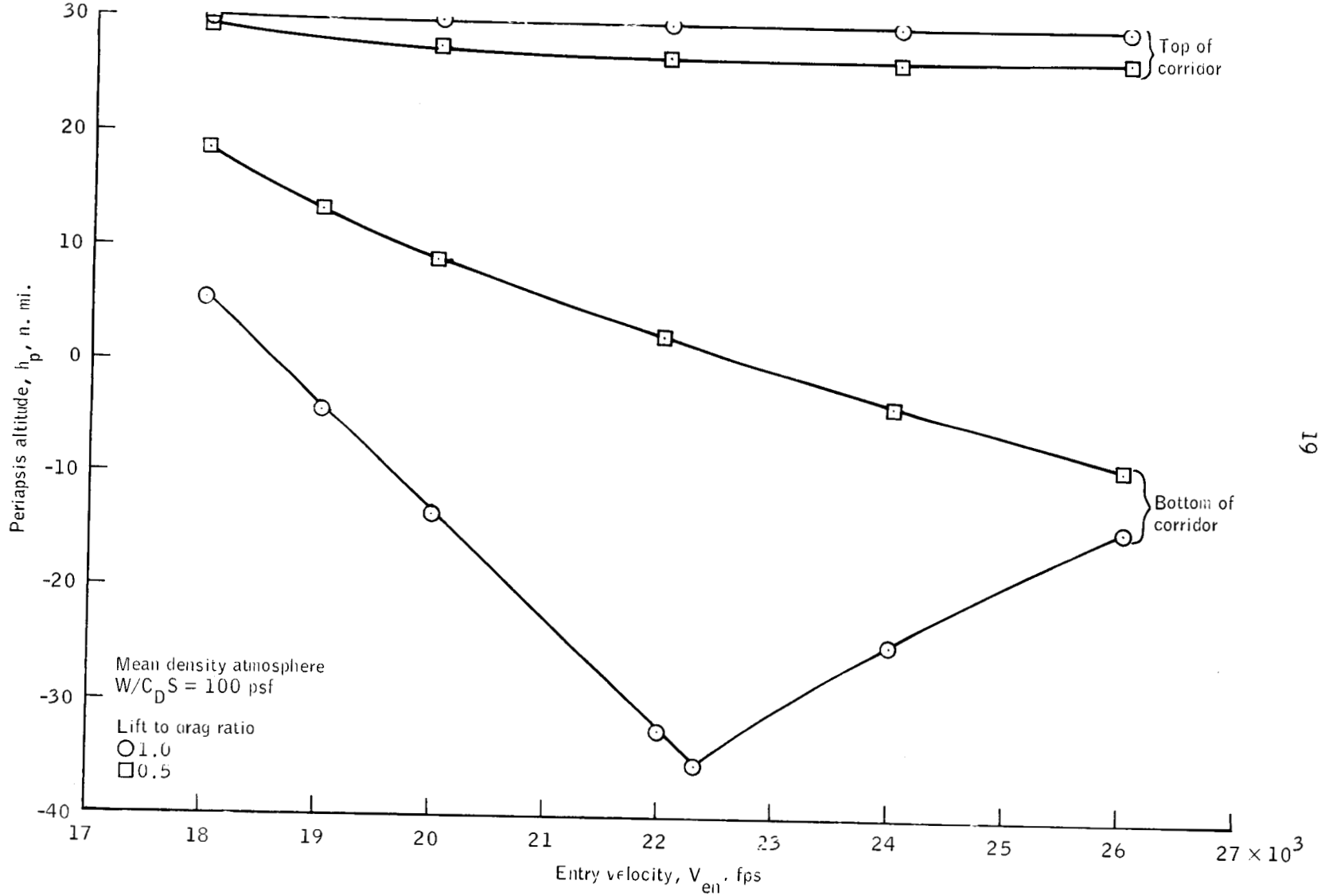

Figure 10.- Effect of reduction in L/D on entry corridor into mean density atmosphere at Mars ($W/C_DS = 100$ psf).

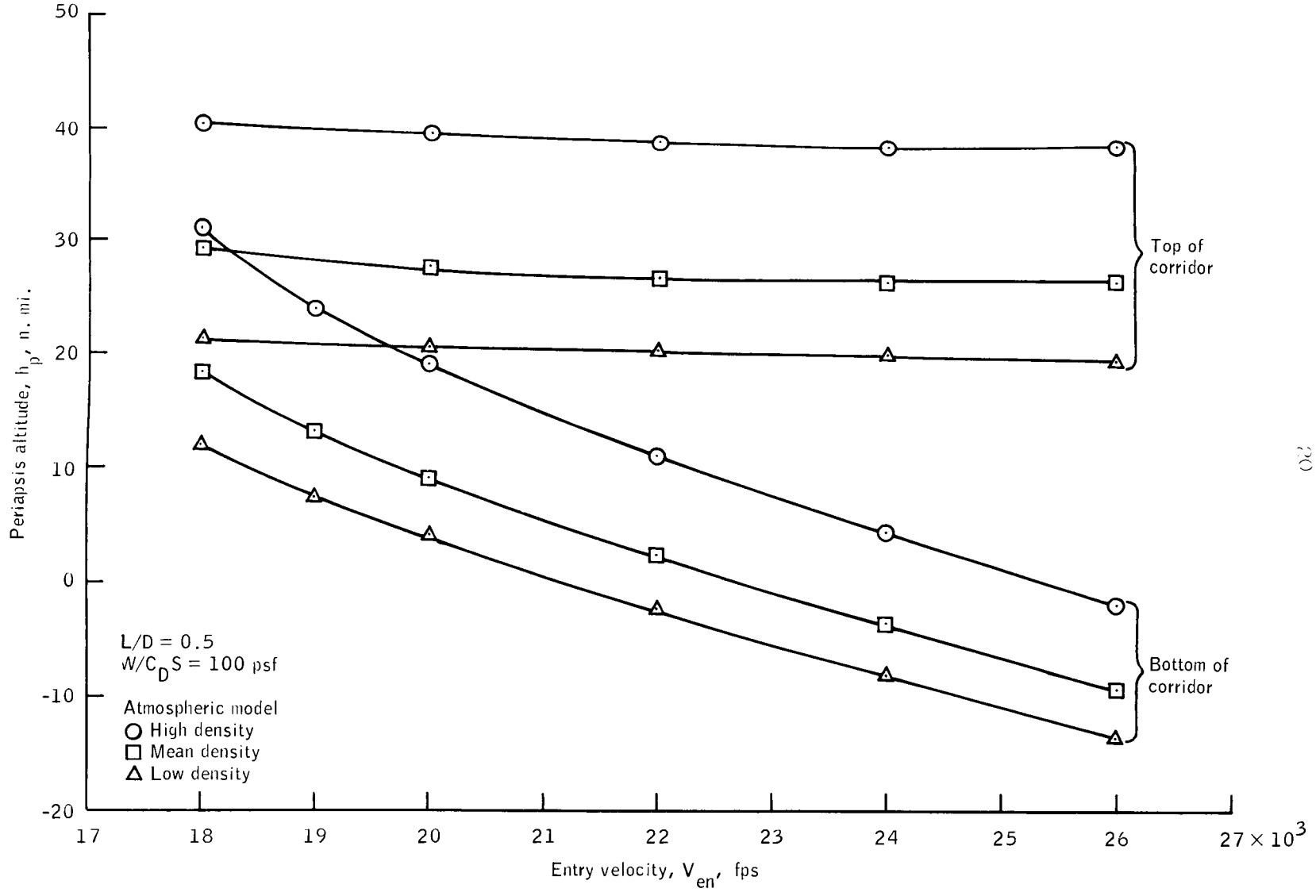

Figure 11.- Entry corridors for three atmospheric models at Mars (L/D = 0.5, W/C_DS = 100 psf).

APPENDIX

GUIDANCE LOGIC

APPENDIX

GUIDANCE LOGIC

The fundamental equations for the guidance were developed in reference 2, and a brief description of the logic is presented in the main text of this report. This appendix includes detailed flow diagrams of the guidance logic and values of the guidance constants.

The only source of information for the guidance equations is the inertial integrating accelerometers which act as the sensing devices. The output of the IMU is the measured change in the velocity along the reference axes. This change in the velocity does not include the effects of gravity. The navigation equations (fig. A-1) are basically identical to those used for the Apollo guidance. They use the measured change in the velocity and calculated effects of gravity to determine the position and velocity of the spacecraft. The measured change in the velocity is also used to estimate the acceleration along the velocity vector (drag acceleration) and to estimate the atmospheric density.

The lift vector of the spacecraft is pointed toward the surface of the planet during the approach phase. The approach phase is defined to end whenever the drag acceleration exceeds $0.05g_E$ where g_E is the gravitational acceleration at the surface of the Earth.

The transition phase (fig. A-2) attempts to guide the spacecraft to a constant altitude path. The density at the beginning of the constant altitude phase is estimated based on the local velocity and an arbitrary value of L/D at the beginning of the constant altitude phase. The estimated density is then used to determine the drag acceleration at the beginning of the constant altitude phase. The value of L/D given by the guidance equation is used except for three cases. The first exception is a result of numerical inaccuracy. The calculated L/D is not used if the estimated density at the beginning of the constant altitude phase is less than the estimated local density. The other two exceptions to the use of the calculated L/D are cases in which the predicted acceleration at the beginning of the constant altitude phase exceeds the acceleration limit and in which the predicted height of the constant altitude path is less than the minimum acceptable altitude. The guidance will command full positive lift if any of these three conditions exist. The transition phase continues until the predicted time remaining before the altitude rate is zero becomes less then the time required to roll the spacecraft through 180°.

The purpose of the constant altitude phase is to permit the spacecraft to decelerate until the exit phase can be flown successfully. Therefore, a portion of the calculations for the exit phase must be performed each cycle although the spacecraft is being guided along a constant altitude path. The exit phase is shown in figures A-3(a) and A-3(b). The constant altitude phase is shown in figure A-4. The purpose of the operations shown in figure A-3(a) is to determine a value of the parameter K which will remain constant for the exit phase and to determine the eccentricity of the exit trajectory. The L/D is decreased until the eccentricity is less than the maximum allowable value or until the L/D is less than some specified value. The latter is one of the conditions which cause the guidance to remain in the constant altitude phase. In figure A-3(b), the apoapsis altitude of the exit trajectory is calculated and compared to the target value. The correct value of the L/D is determined by a combination of a Newton-Raphson iteration scheme and a linear interpolation. The commanded L/D is a combination of the current required value and the previously required value. The guidance escapes from the iteration loop by (1) satisfaction of the target condition, (2) remaining in the iteration loop for 20 cycles, or (3) being unable to keep the eccentricity below a specific value. The constant altitude phase continues until the target apoapsis altitude can be obtained by use of a constant L/D which is less than some specified value.

The lateral logic (fig. A-5) is designed to control the inclination of the exit trajectory plane by a decision as to which quadrants the roll angle should be in. This section is also designed to convert the commanded L/D into a roll angle.

The guidance parameters may be divided into five groups. These general groups are as follows: (1) initial conditions, (2) target conditions, (3) vehicle characteristics, (4) planet characteristics, and (5) guidance constants. These parameters are listed below.

a. Initial conditions

   1. $\underline{r}$, position vector, ft

   2. $\underline{v}$, velocity vector, ft

b. Target conditions

   1. h_{aT}, apoapsis altitude, n. mi.

   2. i_T, inclination, rad

c. Vehicle characteristics

1. $(L/D)_{max}$, maximum L/D

2. B, ballistic coefficient, psf

d. Planet characteristics

1. R, radius, ft

2. μ, gravitational constant, ft^3/sec^2

3. J, oblateness coefficient

4. β, exponential decay rate of density, ft^{-1}

e. Guidance constants

1. a_m, maximum acceleration, $5g_E$

2. D_{thres}, threshold drag acceleration, $0.05g_E$

3. e_{max}, maximum eccentricity, 0.99

4. $h_{a,\ tol}$, tolerance in predicted h_a, 10 n. mi.

5. h_{min}, minimum altitude, 50 000 ft

6. $(L/D)_{ca}$, L/D at beginning of constant altitude phase, $-0.75\ (L/D)_{max}$

7. $(L/D)_{ex}$, maximum L/D during exit phase, 0.35

8. $(L/D)_{ex,\ m}$, minimum L/D during exit phase, 0.09

9. K_{tol}, tolerance in K, 10^{-5}

10. K_3, guidance gains, 0.01

11. K_4, 100

12. K_5, 10

13. LDBIAS, 0.5

14. LADBI2, 4.0

15. δi, tolerance in inclination, 0.5°

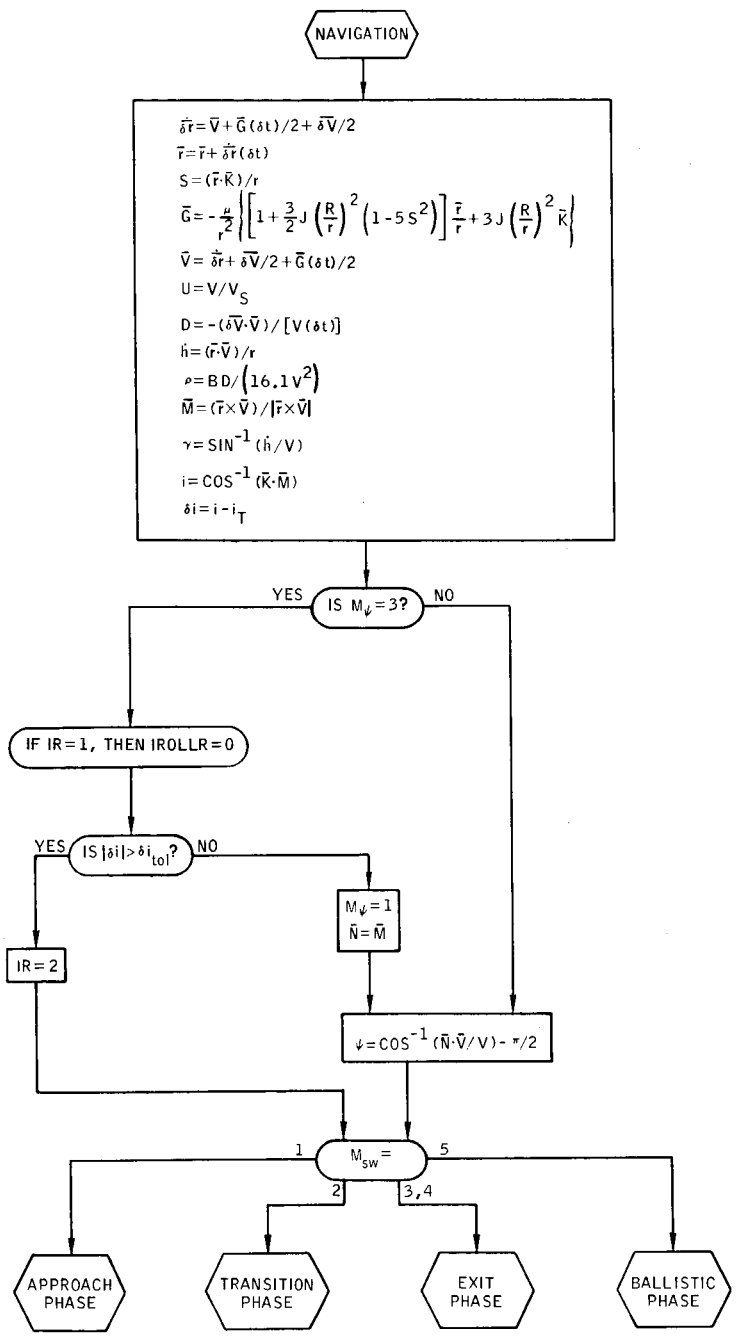

Figure A1. - Navigation section.

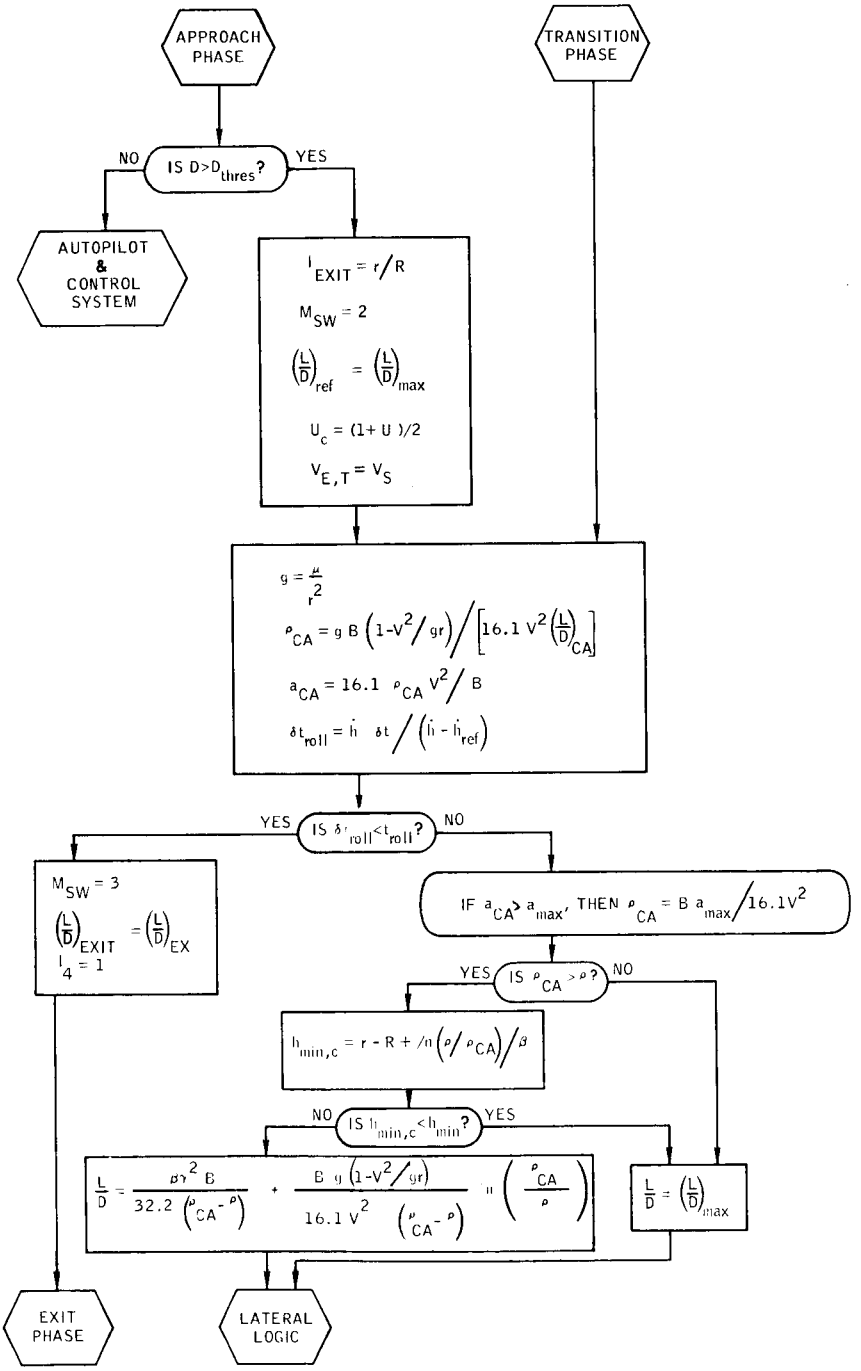

Figure A2.- Approach and transition phases.

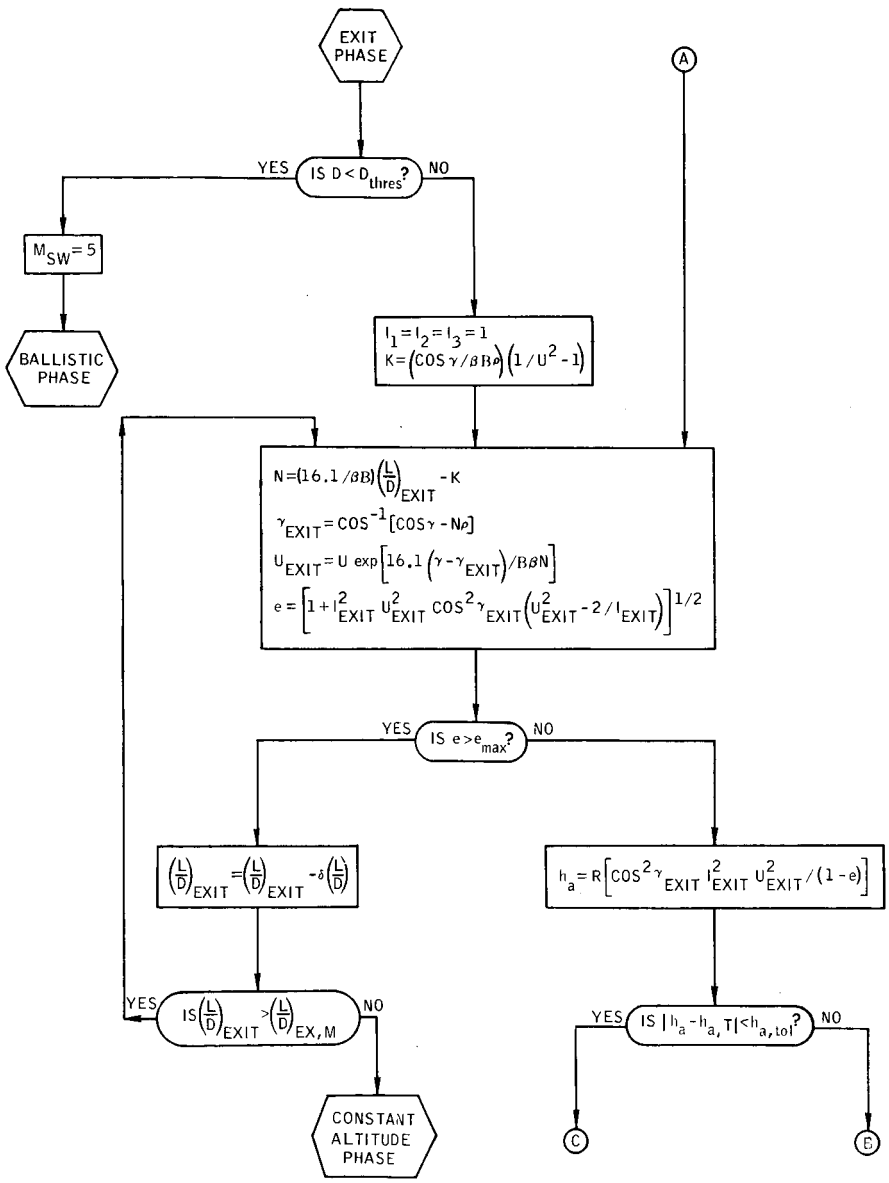

Figure A3.- Exit phase.

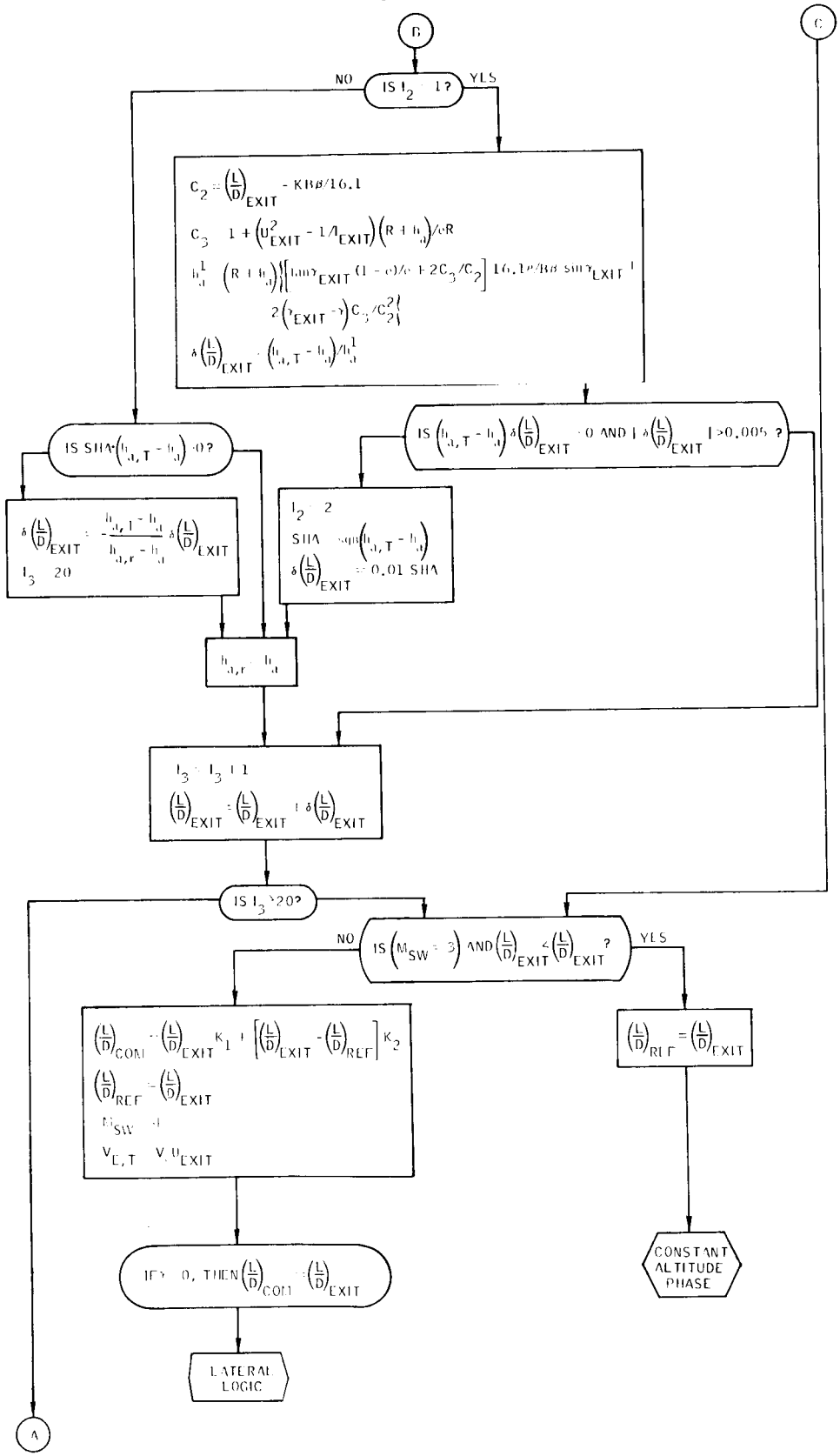

FIGURE A3.- CONCLUDED

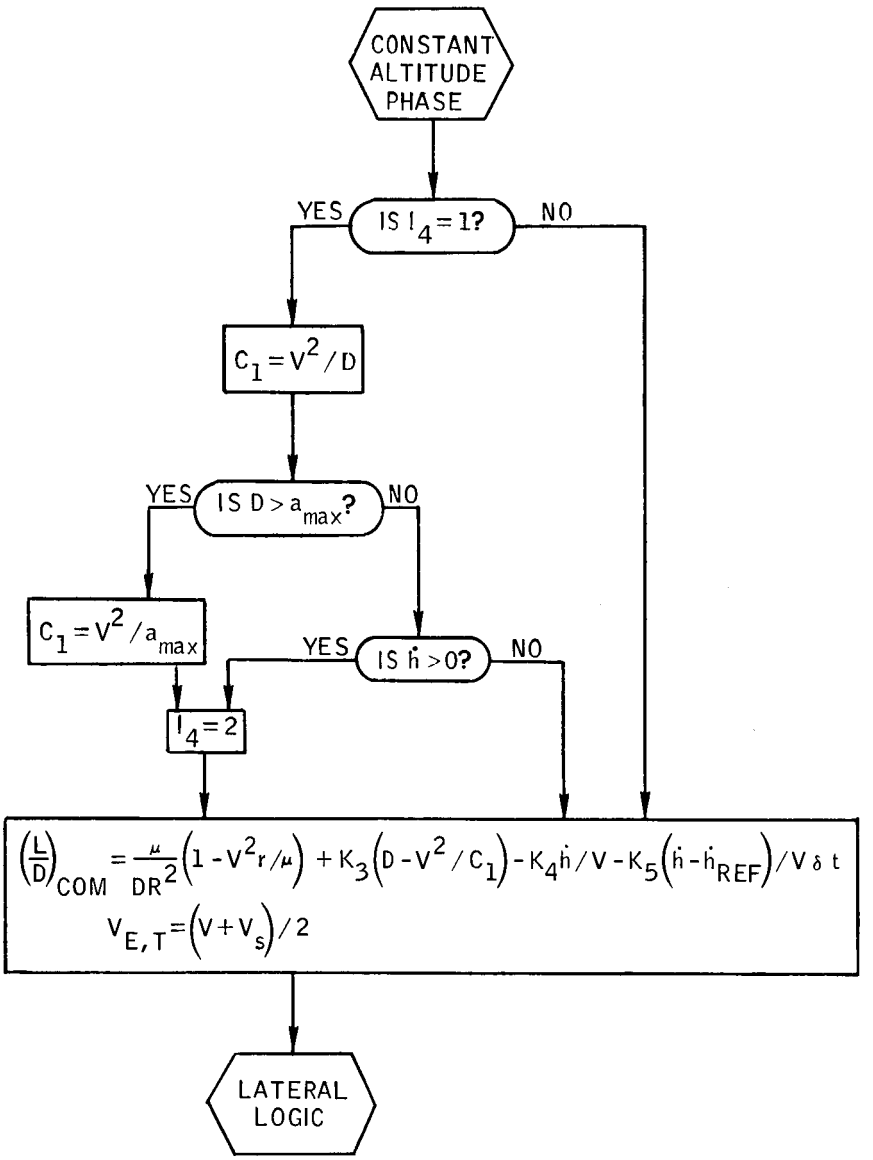

Figure A4.- Constant altitude phase.

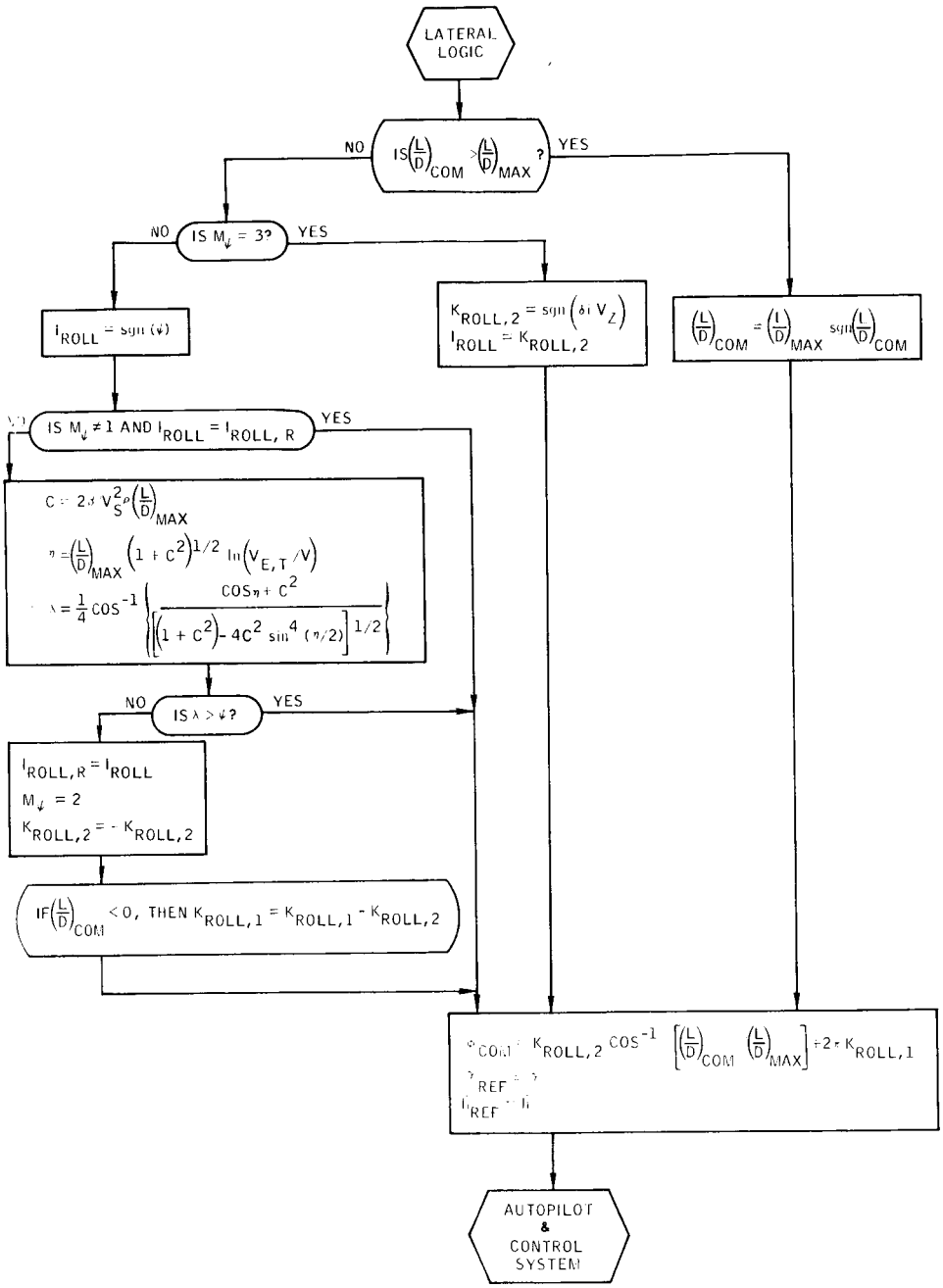

FIGURE A5.- LATERAL LOGIC

REFERENCES

1. Repic, E. M.; Boobar, M. G.; and Chapel, F. G.: Aerobraking as a Potential Planetary Capture Mode. Journal of Spacecraft and Rockets, Vol. 5, No. 8, August 1968, pp.921-926.

2. Garland, Benjamine J.: Guidance Analysis of Aerodynamics Braking into Orbit Around Mars. MSC IN 68-FM-244, October 3, 1968.

3. Martin, F. H.; and Battin, R. H.: Computer-Controlled Steering of the Apollo Spacecraft. Journal of Spacecraft and Rockets Volume 5, No. 4, April 1968, pp. 400-407

4. White, Jack A.: Feasibility Study of a Bang-Bang Path Control for a Reentry Vehicle. NASA TN-D-2049, November 1963.

5. Loh, W. H. T.: Extension of the Second-Order Theory of Entry Mechanics to Oscillatory Entry Solutions, AIAA Journal, Volume 3, No. 9, September 1965, pp. 1688-1691.

6. Wang, H. E.: Motion of Re-Entry Vehicles During Constant-Altitude Glide. AIAA Journal, Volume 3, No. 7, July 1965, pp. 1346-1347.

7. Michaux, C. M.: Handbook of the Physical Properties of the Planet Mars. NASA SP-2070, 1967.

8. Koenig, L. R; Murray, F. W.; Michaux, C. M.; and Hyatt, H. A.: Handbook of the Physical Properties of the Planet Venus. NASA SP-3029, 1967.

9. Models of Mars Atmosphere (1967). NASA SP-8010, May 1968.

10. Models of Venus Atmosphere (1968). NASA SP-8011, December 1968.

11. Boobar, M. G.; Repic, E. M.; and McDermott, A. M.: Approach and Entry Corridors for Aerobraking at Mars and Venus. Journal of Spacecraft and Rockets Volume 4, No. 5, May 1967, pp. 682-684.